Adaptive Subspace Tests for Multichannel Signal Detection in Auto-Regressive Disturbance

Yongchan Gao, *Member, IEEE*, Hongbin Li, *Senior Member, IEEE*, and Braham Himed, *Fellow, IEEE*

***Abstract*—This paper deals with the problem of detecting a subspace signal in the presence of spatially and temporally colored disturbance. A new subspace parametric signal model that takes into account a multi-rank subspace structure for the target signal and employs a multi-channel auto-regressive process for the disturbance signal is proposed. Following this model, a new subspace parametric Rao detector (SP-Rao) is developed for training-limited scenarios. Unlike conventional parametric detectors that are designed for only rank-one signal detection, the SP-Rao has a new multi-rank structure with a pairwise successive spatio-temporal whitening and cross-correlation process between the observed signal and each subspace basis vector. Additionally, a non-parametric subspace detector (NSD) is derived based upon a frequency-domain representation of the SP-Rao test statistic. The NSD is distinctively different from conventional subspace detectors, in which the former involves pairwise whitening and cross-correlation between the test signal and each subspace basis vector but the latter employs the whole subspace matrix. Numerical results are presented to illustrate the performance of the proposed subspace detectors in comparison with several leading existing methods, especially in the case of limited data.**

***Index Terms*—Adaptive signal detection, subspace signal detection, Rao test, multi-channel auto-regressive model, space-time adaptive processing.**

I. Introduction

MULTI-CHANNEL adaptive signal detection is a fundamental problem in radar, sonar, wireless communications, and other applications. Adaptive detection of a rank-one signal has been extensively studied; see, e.g., [1]–[3] and references therein. One limitation of rank-one signal detection techniques is that they rely on knowledge of the exact steering vector or the rank-one structure of the target signal. In practical applications, mismatches of the signal steering vector may exist due to imperfect antenna shape, calibration and pointing errors, and wavefront distortions [4], [5]. Besides, the signal of interest is inherently multi-rank in some practical applications, such as target detection using data collected from multiple polarimetric channels [6], multiuser detection [7], and signal estimation in multipath environments [8]. Therefore, it is necessary to consider subspace signal detection by accounting for uncertainties of the actual signal steering vector as well as multi-rank targets.

Here, a subspace signal refers to a multichannel signal that lies in a subspace with unknown coordinates. The rank of a subspace signal is the dimension of the subspace that the signal belongs to. A subspace signal can be used to model the uncertainty of the actual signal steering vector as well as natural multi-rank targets. A number of detection problems may be formulated by using the subspace signal model. Taking space-time adaptive processing (STAP) as an example, the detection of a target at a given bearing and with a radial velocity within a prescribed set of values to account either for target acceleration during the coherent observation interval or for uncertainty in the target Doppler, may be formulated as a subspace detection problem [9]. A multitude of subspace signal detection algorithms have been introduced, including the generalized likelihood ratio test (GLRT) [10], the adaptive matched filter (AMF) [6], the Rao test [11], and others [12]–[14].

Typically, a large amount of training data is required for adaptive detection to estimate the unknown correlation of the disturbance signal. Specifically, the number of training samples required for estimating the disturbance covariance matrix for an acceptable performance needs be at least twice the system spatio-temporal dimensionality to ensure acceptable detection performance [15]. Such a large training requirement cannot be met in some applications due to the presence of strong discrete scatterers, terrain type variations, and system configurations [2]. As a result, the lack of adequate training support limits the performance of conventional receivers.

To alleviate the problem of excessive training data requirement, a number of techniques have been investigated. The knowledge-aided approach, which incorporates a priori information of the disturbance for adaptive processing, can reduce the sample support, either by directly exploiting the a priori knowledge [16], or by indirectly modeling the covariance matrix as a random matrix with some prior distribution using a Bayesian framework [17]–[19]. Additionally, the persymmetric structure of the disturbance covariance matrix has been employed for performance improvements in training-limited scenarios [20]–[24]. Specifically, when the radar system utilizes an antenna array with linear symmetrically spaced elements and/or uniformly spaced pulse trains, the covariance matrix exhibits a persymmetric structure, which can be utilized to reduce

Manuscript received April 24, 2018; revised August 6, 2018; accepted August 29, 2018. Date of publication September 10, 2018; date of current version September 24, 2018. The associate editor coordinating the review of this manuscript and approving it for publication was Dr. Gang Li. This work was supported by the National Science Foundation under Grant ECCS-1609393. *(Corresponding author: Hongbin Li.)*

Y. Gao and H. Li are with the Department of Electrical and Computer Engineering, Stevens Institute of Technology, Hoboken, NJ 07030 USA (e-mail: yongchangao@gmail.com; hli@stevens.edu).

B. Himed is with the AFRL/RYMD, Dayton, OH 45433 USA (e-mail: braham.himed@us.af.mil).

Color versions of one or more of the figures in this paper are available online at http://ieeexplore.ieee.org.

Digital Object Identifier 10.1109/TSP.2018.2869123

the training requirement [20]. Also, several recent studies have explored the clutter symmetry for training reduction [25]–[27]. For instance, ground clutter observed by a stationary monostatic radar often exhibits a symmetric power spectral density structure around the zero-Doppler frequency. Exploiting the clutter symmetry can reduce the number of nuisance parameters that need to be estimated at the design stage.

The parametric approach is another way to reduce training requirements. Parametric methods that model the disturbance signal as a multi-channel auto-regressive (AR) process have been considered for airborne radar detection with proven success using measured STAP datasets [28], [29]. Examples of parametric detectors are the parametric AMF (PAMF) [28], [29], the parametric Rao (PRao) test [30], and the parametric GLRT (PGLRT) [31]. Variants of parametric detection are also examined in [32]–[34].

In this paper, we consider subspace detection when the correlation structure of the disturbance can be captured by a multichannel AR process, and develop two new subspace detectors, both of which are suitable for multi-rank subspace signal detection in training-limited scenarios. First, we propose a new subspace parametric signal model that takes into account the multi-rank subspace structure of the signal of interest and the spatio-temporal correlation of the disturbance using a multichannel AR process. Following this model, we propose a subspace parametric Rao detector (SP-Rao) that is distinctively different from conventional parametric detectors that are designed for rank-one only signal detection. Specifically, the test statistic of the SP-Rao has a new multi-rank structure that involves a pairwise successive spatio-temporal whitening and cross-correlation between the observed signal and each subspace basis vector. The second detector, referred to as the non-parametric subspace detector (NSD), is derived via a frequency-domain representation of the SP-Rao test variable. Unlike traditional subspace detectors that perform matched filtering using the complete subspace matrix, the NSD performs pairwise whitening and cross-correlation using individual subspace basis vectors. Numerical results show that the proposed subspace detectors can achieve significantly enhanced detection performance over conventional detectors when the amount of training data is limited.

The remainder of this paper is organized as follows. The signal model is presented in Section II. The proposed detectors for subspace signal detection are derived in Section III. Numerical results are provided in Section IV. Finally, conclusions are given in Section V.

Notation: Vectors (matrices) are denoted by boldface lower (upper) case letters. Superscripts $(\cdot)^*$, $(\cdot)^T$, and $(\cdot)^\dagger$ denote conjugate, transpose, and conjugate transpose, respectively. $\mathrm{tr}(\cdot)$ indicates the trace of a matrix. $|\cdot|$ with a square matrix argument represents the determinant of that matrix, and $|\cdot|$ with a complex number represents the modulus. $E\{\cdot\}$ denotes the expectation operator and $j=\sqrt{-1}$. $\otimes$ denotes the Kronecker product, and $\mathrm{vec}(\cdot)$ denotes the operation of stacking the columns of a matrix on top of each other. $\langle\cdot\rangle$ denotes the subspace spanned by columns of a matrix. $\Re\{\cdot\}$ denotes the real part and $\Im\{\cdot\}$ denotes the imaginary part. The notation $\mathcal{CN}$ denotes the complex Gaussian distribution.

II. Signal Model

Consider detecting a target signal that lies in a subspace spanned by the columns of an $NJ\times r$ full-rank matrix $\mathbf{H}$, where $\mathbf{H}=[\mathbf{h}_1,\ldots,\mathbf{h}_r]$, J denotes the number of spatial channels, N is the number of temporal observations, and r denotes the rank of the subspace signal. The test signal $\mathbf{x}_0(n)$ under the alternative hypothesis is

$$\mathbf{x}_0(n)=\sum_{i=1}^{r}\alpha_i\mathbf{h}_i(n)+\mathbf{d}_0(n),\ n=0,\ldots,N-1, \tag{1}$$

where α_i is the ith element of the unknown target amplitude $\boldsymbol{\alpha}=[\alpha_1,\ldots,\alpha_r]^T$, $\mathbf{d}_0(n)$ is the disturbance signal that is assumed to be correlated in space and time, and $\mathbf{h}_i(n)$ denotes the nth $J\times 1$ subvector of the ith column vector $\mathbf{h}_i$. In practice, the covariance matrix of the disturbance signal is usually unknown. A standard assumption is the availability of a set of target-free training data

$$\mathbf{x}_k(n)=\mathbf{d}_k(n),\ k=1,\ldots,K, \tag{2}$$

where K is the size of training samples.

Denote the null hypothesis (H_0) as the case where the test data is target-free and the alternative hypothesis (H_1) as the case where the test data contains the target signal. The problem of detecting a subspace signal in the presence of spatially and temporally correlated disturbance can then be formulated as the following binary hypothesis testing problem:

$$\begin{aligned} H_0:&\begin{cases}\mathbf{x}_0(n)=\mathbf{d}_0(n),\ n=0,\ldots,N-1\\ \mathbf{x}_k(n)=\mathbf{d}_k(n),\ k=1,\ldots,K;\end{cases}\\ H_1:&\begin{cases}\mathbf{x}_0(n)=\sum_{i=1}^{r}\alpha_i\mathbf{h}_i(n)+\mathbf{d}_0(n),\ n=0,\ldots,N-1\\ \mathbf{x}_k(n)=\mathbf{d}_k(n),\ k=1,\ldots,K.\end{cases}\end{aligned} \tag{3}$$

Denote the columns of the subspace matrix, disturbance signals, and the received signals as

$$\begin{aligned}\mathbf{h}_i&=[\mathbf{h}_i^T(0),\mathbf{h}_i^T(1),\ldots,\mathbf{h}_i^T(N-1)]^T\\ \mathbf{d}_k&=[\mathbf{d}_k^T(0),\mathbf{d}_k^T(1),\ldots,\mathbf{d}_k^T(N-1)]^T\\ \mathbf{x}_k&=[\mathbf{x}_k^T(0),\mathbf{x}_k^T(1),\ldots,\mathbf{x}_k^T(N-1)]^T.\end{aligned} \tag{4}$$

Then, the adaptive detection problem (3) can be rewritten in the following compact form

$$\begin{aligned} H_0:&\begin{cases}\mathbf{x}_0=\mathbf{d}_0\\ \mathbf{x}_k=\mathbf{d}_k,\ k=1,\ldots,K;\end{cases}\\ H_1:&\begin{cases}\mathbf{x}_0=\mathbf{H}\boldsymbol{\alpha}+\mathbf{d}_0\\ \mathbf{x}_k=\mathbf{d}_k,\ k=1,\ldots,K.\end{cases}\end{aligned} \tag{5}$$

It is assumed that the disturbance signals $\mathbf{d}_k, k=0,\ldots,K$ are independent and identically distributed (i.i.d.) with the complex Gaussian distribution; i.e., $\mathbf{d}_k\sim\mathcal{CN}(\mathbf{0},\mathbf{R})$, where $\mathbf{R}$ is the unknown space-time covariance matrix.

Under the parametric framework, the disturbance signals $\mathbf{d}_k(n), k=0,\ldots,K$ are further assumed to follow the

J-channel AR process

$$\mathbf{d}_k(n) = -\sum_{p=1}^{P} \mathbf{A}^{\dagger}(p)\mathbf{d}_k(n-p) + \boldsymbol{\varepsilon}_k(n), \tag{6}$$

where $\left\{\mathbf{A}^{\dagger}(p)_{p=1}^{P}\right\}$ denote the unknown $J \times J$ AR coefficient matrices, P is the model order, and $\boldsymbol{\varepsilon}_k(n)$ denotes the $J \times 1$ spatial noise vectors that are temporally white but spatially colored, namely, $\boldsymbol{\varepsilon}_k(n) \sim \mathcal{CN}(\mathbf{0}, \mathbf{Q}), k = 0, \ldots, K$, with an unknown $J \times J$ spatial covariance matrix $\mathbf{Q}$.

Some discussions on the multichannel AR model for the disturbance signal are in order. In radar systems, the disturbance typically includes clutter and noise, which are known to exhibit spatial and temporal correlation [15]. The correlation is usually described by the $NJ \times NJ$ space-time covariance $\mathbf{R}$ that needs to be estimated from training data. When N and J are large, the estimation entails a large amount of training data that may be difficult to obtain in practice. To address this issue, multichannel AR models have been identified as useful tools to represent radar disturbance signals [35]. Such models have been extensively tested using experimentally collected data and successfully employed to model, e.g., ground [36] and sea clutter [37] in ground based radar systems, as well as disturbances in airborne radar systems [29], [38]. The model order P, which is usually unknown, can be estimated by standard model order selection techniques, such as the Akaike information criterion (AIC) and the minimum description length (MDL) criterion [39]. A potential downside of the model-based approach is model mismatch, i.e., when the model order P is incorrectly estimated. Fortunately, for most real-world radar clutter representation, the model order P is small [29], which implies that the mismatch is likely to be small. It was found in [40] that a small model mismatch, especially with an over-estimated the model order, has only minor impact on the radar detection performance.

Following the parametric model, we have

$$\begin{aligned}&\mathbf{x}_0(n) - \sum_{i=1}^{r} \alpha_i \mathbf{h}_i(n) \\ &= -\sum_{p=1}^{P} \mathbf{A}^{\dagger}(p) \left[\mathbf{x}_0(n-p) - \sum_{i=1}^{r} \alpha_i \mathbf{h}_i(n-p)\right] + \boldsymbol{\varepsilon}_0(n).\end{aligned} \tag{7}$$

Let $\tilde{\mathbf{h}}_i(n)$ denote a regression on $\mathbf{h}_i(n)$ and $\tilde{\mathbf{x}}_0$ a regression on $\mathbf{x}_0$ under H_1 as follows, which represent the temporally whitened steering vector and test signal, respectively

$$\tilde{\mathbf{h}}_i(n) = \mathbf{h}_i(n) + \sum_{p=1}^{P} \mathbf{A}^{\dagger}(p)\mathbf{h}_i(n-p), \tag{8}$$

$$\tilde{\mathbf{x}}_0(n) = \mathbf{x}_0(n) + \sum_{p=1}^{P} \mathbf{A}^{\dagger}(p)\mathbf{x}_0(n-p). \tag{9}$$

Note that for $r > 1$ the target signal in the test data $\mathbf{x}_0(n)$ belongs to the subspace $\langle \mathbf{H} \rangle$, and this multi-rank subspace model can account for uncertainties in the signal steering vector as well as natural multi-rank signal structures that are found in, e.g., polarization radar returns. On the other hand, the parametric detectors developed in [28]–[31] cannot be applied to the multi-rank subspace detection problem (3), since they are designed for rank-one signal detection.

III. The Proposed Detectors

The optimum solution to the hypothesis testing problem (3) is the likelihood ratio test in terms of the Neyman-Pearson criterion. However, this procedure does not lead to a uniformly most powerful (UMP) test and a possible alternative is to resort to the GLRT, which is tantamount to replacing the unknown parameters by their maximum likelihood (ML) estimates under each hypothesis. Unfortunately, the decision statistic based on the GLRT for the problem (3) does not generally admit a closed-form expression. Thus, we consider instead the Rao test. In the following, we will devise two adaptive subspace detectors.

A. Adaptive Subspace Parametric Rao Test (SP-Rao)

Denote all unknown parameters as

$$\boldsymbol{\theta} = \begin{bmatrix} \boldsymbol{\theta}_r \\ \boldsymbol{\theta}_s \end{bmatrix}, \tag{10}$$

where $\boldsymbol{\theta}_r = [\Re(\boldsymbol{\alpha}^T), \Im(\boldsymbol{\alpha}^T)]^T$ denotes the signal parameter vector, $\boldsymbol{\theta}_s = [\mathbf{q}_R^T, \mathbf{q}_I^T, \mathbf{a}_R^T, \mathbf{a}_I^T]^T$ denotes the nuisance parameter vector. Here, $\mathbf{a}_R = \mathrm{vec}(\Re(\mathbf{A}))$, $\mathbf{a}_I = \mathrm{vec}(\Im(\mathbf{A}))$, $\mathbf{q}_R^T$ contains the diagonal elements and the real part of the elements on and below the diagonal in $\mathbf{Q}$, and $\mathbf{q}_I^T$ contains the imaginary part of the elements below the diagonal in $\mathbf{Q}$. Moreover, we use $\hat{\boldsymbol{\theta}}_0 = [\hat{\boldsymbol{\theta}}_{r0}, \hat{\boldsymbol{\theta}}_{s0}]$ to denote the ML estimate of $\boldsymbol{\theta}$ under H_0.

The Rao test is given by [41]

$$\left.\frac{\partial \ln f(\boldsymbol{\theta})}{\partial \boldsymbol{\theta}_r}\right|_{\boldsymbol{\theta}=\hat{\boldsymbol{\theta}}_0}^{T} [\mathbf{I}^{-1}(\hat{\boldsymbol{\theta}}_0)]_{\boldsymbol{\theta}_r,\boldsymbol{\theta}_r} \left.\frac{\partial \ln f(\boldsymbol{\theta})}{\partial \boldsymbol{\theta}_r}\right|_{\boldsymbol{\theta}=\hat{\boldsymbol{\theta}}_0} \underset{H_0}{\overset{H_1}{\gtrless}} \xi, \tag{11}$$

where

- the Fisher information matrix $\mathbf{I}(\boldsymbol{\theta})$ is expressed as

$$\mathbf{I}(\boldsymbol{\theta}) = \begin{bmatrix} \mathbf{I}_{\boldsymbol{\theta}_r,\boldsymbol{\theta}_r}(\boldsymbol{\theta}) & \mathbf{I}_{\boldsymbol{\theta}_r,\boldsymbol{\theta}_s}(\boldsymbol{\theta}) \\ \mathbf{I}_{\boldsymbol{\theta}_s,\boldsymbol{\theta}_r}(\boldsymbol{\theta}) & \mathbf{I}_{\boldsymbol{\theta}_s,\boldsymbol{\theta}_s}(\boldsymbol{\theta}) \end{bmatrix} \tag{12}$$

  with

$$\begin{aligned}[\mathbf{I}^{-1}(\boldsymbol{\theta})]_{\boldsymbol{\theta}_r,\boldsymbol{\theta}_r} = [&\mathbf{I}_{\boldsymbol{\theta}_r,\boldsymbol{\theta}_r}(\boldsymbol{\theta}) - \mathbf{I}_{\boldsymbol{\theta}_r,\boldsymbol{\theta}_s}(\boldsymbol{\theta})\mathbf{I}^{-1}_{\boldsymbol{\theta}_s,\boldsymbol{\theta}_s} \\ &(\boldsymbol{\theta})\mathbf{I}_{\boldsymbol{\theta}_s,\boldsymbol{\theta}_r}(\boldsymbol{\theta})]^{-1};\end{aligned} \tag{13}$$

- the joint probability density function (PDF) of the test and training data $f(\boldsymbol{\theta})$ is

$$f(\boldsymbol{\theta}) = \left\{\frac{1}{\pi^J |\mathbf{Q}|} \exp\{-\mathrm{tr}[\mathbf{Q}^{-1}\mathbf{T}(\boldsymbol{\alpha}, \mathbf{A})]\}\right\}^{(K+1)(N-P)} \tag{14}$$

  with

$$\mathbf{T}(\boldsymbol{\alpha}, \mathbf{A}) = \frac{\sum_{n=P}^{N-1} \boldsymbol{\varepsilon}_0(n)\boldsymbol{\varepsilon}_0^{\dagger}(n) + \sum_{k=1}^{K}\sum_{n=P}^{N-1} \boldsymbol{\varepsilon}_k(n)\boldsymbol{\varepsilon}_k^{\dagger}(n)}{(K+1)(N-P)}, \tag{15}$$

$$\boldsymbol{\varepsilon}_0(n) = \tilde{\mathbf{x}}_0(n) - \sum_{i=1}^{r} \alpha_i \tilde{\mathbf{h}}_i(n), \tag{16}$$

and

$$\boldsymbol{\varepsilon}_k(n) = \mathbf{x}_k(n) + \sum_{p=1}^{P} \mathbf{A}^{\dagger}(p)\mathbf{x}_k(n-p); \tag{17}$$

- ξ denotes the threshold.

To derive the test (11), we first evaluate the first partial derivatives of the log likelihood and $[\mathbf{I}^{-1}(\boldsymbol{\theta})]_{\boldsymbol{\theta}_r,\boldsymbol{\theta}_r}$ for the nuisance parameters. The first partial derivative of the log likelihood function with respect to (w.r.t.) $\boldsymbol{\theta}_r$ is

$$\frac{\partial \ln f(\boldsymbol{\theta})}{\partial \boldsymbol{\theta}_r} = \begin{bmatrix} \dfrac{\partial \ln f(\boldsymbol{\theta})}{\partial \boldsymbol{\alpha}_R} \\ \dfrac{\partial \ln f(\boldsymbol{\theta})}{\partial \boldsymbol{\alpha}_I} \end{bmatrix}. \tag{18}$$

where

$$\frac{\partial \ln f(\boldsymbol{\theta})}{\partial \boldsymbol{\alpha}_R} = \left[\frac{\partial \ln f}{\partial \alpha_{R,1}}, \ldots, \frac{\partial \ln f}{\partial \alpha_{R,r}}\right]^T,$$
$$\frac{\partial \ln f(\boldsymbol{\theta})}{\partial \boldsymbol{\alpha}_I} = \left[\frac{\partial \ln f}{\partial \alpha_{I,1}}, \ldots, \frac{\partial \ln f}{\partial \alpha_{I,r}}\right]^T \tag{19}$$

with

$$\begin{aligned}\frac{\partial \ln f}{\partial \alpha_{R,i}} &= \sum_{n=P}^{N-1} \tilde{\mathbf{h}}_i^{\dagger}(n)\mathbf{Q}^{-1}\boldsymbol{\varepsilon}_0(n) + \sum_{n=P}^{N-1} \boldsymbol{\varepsilon}_0^{\dagger}(n)\mathbf{Q}^{-1}\tilde{\mathbf{h}}_i(n) \\ &= \sum_{n=P}^{N-1} \tilde{\mathbf{h}}_i^{\dagger}(n)\mathbf{Q}^{-1}\left[\tilde{\mathbf{x}}_0(n) - \sum_{m=1}^{r} \alpha_m \tilde{\mathbf{h}}_m(n)\right] \\ &\quad + \sum_{n=P}^{N-1} \left[\tilde{\mathbf{x}}_0(n) - \sum_{m=1}^{r} \alpha_m \tilde{\mathbf{h}}_m(n)\right]^{\dagger} \mathbf{Q}^{-1}\tilde{\mathbf{h}}_i(n)\end{aligned} \tag{20}$$

and

$$\frac{\partial \ln f}{\partial \alpha_{I,i}} = j\sum_{n=P}^{N-1} \tilde{\mathbf{h}}_i^{\dagger}(n)\mathbf{Q}^{-1}\boldsymbol{\varepsilon}_0(n) - \sum_{n=P}^{N-1} \boldsymbol{\varepsilon}_0^{\dagger}(n)\mathbf{Q}^{-1}\tilde{\mathbf{h}}_i(n). \tag{21}$$

The derivation of $\mathbf{I}(\boldsymbol{\theta})_{\boldsymbol{\theta}_r,\boldsymbol{\theta}_r}$ is shown in Appendix A. Therefore, $[\mathbf{I}^{-1}(\boldsymbol{\theta})]_{\boldsymbol{\theta}_r,\boldsymbol{\theta}_r}$ is given by (22) shown at the bottom of this page. Then, substituting (18) and (22) into (11) yields (23) as shown at the bottom of this page.

Now we find the ML estimates of the nuisance parameters under H_0, which are needed by the test (11). The ML estimates of $\mathbf{Q}$ and $\mathbf{A}$ are given by (see Appendix B for details)

$$\hat{\mathbf{A}} = -\hat{\mathbf{R}}_{yy}^{-1}\hat{\mathbf{R}}_{yx} \tag{24}$$

and

$$\hat{\mathbf{Q}} = \frac{\hat{\mathbf{R}}_{xx} - \hat{\mathbf{R}}_{yx}^{\dagger}\hat{\mathbf{R}}_{yy}^{-1}\hat{\mathbf{R}}_{yx}}{(K+1)(N-P)}, \tag{25}$$

where $\hat{\mathbf{R}}_{xx}$, $\hat{\mathbf{R}}_{yy}$, and $\hat{\mathbf{R}}_{yx}$ are defined in (62), (63), and (64) of Appendix A.

Finally, substituting (24) and (25) into (23) yields the subspace parametric Rao detector

$$\Lambda = \sum_{\ell=1}^{r}\sum_{i=1}^{r} \frac{\left(\sum_{n=P}^{N-1} \hat{\tilde{\mathbf{x}}}_0(n)^{\dagger}\hat{\mathbf{Q}}^{-1}\hat{\tilde{\mathbf{h}}}_i(n)\right)\left(\sum_{n=P}^{N-1} \hat{\tilde{\mathbf{h}}}_\ell(n)^{\dagger}\hat{\mathbf{Q}}^{-1}\hat{\tilde{\mathbf{x}}}_0(n)\right)}{\sum_{n=P}^{N-1} \hat{\tilde{\mathbf{h}}}_i(n)^{\dagger}\hat{\mathbf{Q}}^{-1}\hat{\tilde{\mathbf{h}}}_\ell(n)} \tag{26}$$

where

$$\hat{\tilde{\mathbf{h}}}_i(n) = \mathbf{h}_i(n) + \sum_{p=1}^{P} \hat{\mathbf{A}}^{\dagger}(p)\mathbf{h}_i(n-p), \tag{27}$$

$$\hat{\tilde{\mathbf{x}}}_0(n) = \mathbf{x}_0(n) + \sum_{p=1}^{P} \hat{\mathbf{A}}^{\dagger}(p)\mathbf{x}_0(n-p). \tag{28}$$

It should be noted that each individual term inside the sum of (26)

$$t_{\ell,i} = \frac{\left(\sum_{n=P}^{N-1} \hat{\tilde{\mathbf{x}}}_0(n)^{\dagger}\hat{\mathbf{Q}}^{-1}\hat{\tilde{\mathbf{h}}}_i(n)\right)\left(\sum_{n=P}^{N-1} \hat{\tilde{\mathbf{h}}}_\ell(n)^{\dagger}\hat{\mathbf{Q}}^{-1}\hat{\tilde{\mathbf{x}}}_0(n)\right)}{\sum_{n=P}^{N-1} \hat{\tilde{\mathbf{h}}}_i(n)^{\dagger}\hat{\mathbf{Q}}^{-1}\hat{\tilde{\mathbf{h}}}_\ell(n)} \tag{29}$$

is not necessarily real. It is real-valued for $\ell = i$, and complex-valued for $\ell \neq i$. Recall that the test statistics Λ is real-valued and compared with a real-valued threshold. Thus, it is helpful to rewrite (26) in a real form. To this end, we divide the index matrix for (ℓ, i) into three groups depending on the relative values of the indices ℓ and i: $\ell = i$, $\ell < i$, and $\ell > i$. Then, let

$$\begin{cases} t_i^{(1)} = \sum_{n=P}^{N-1} \hat{\tilde{\mathbf{x}}}_0(n)^{\dagger}\hat{\mathbf{Q}}^{-1}\hat{\tilde{\mathbf{h}}}_i(n) \\ t_\ell^{(2)} = \sum_{n=P}^{N-1} \hat{\tilde{\mathbf{h}}}_\ell(n)^{\dagger}\hat{\mathbf{Q}}^{-1}\hat{\tilde{\mathbf{x}}}_0(n) \\ t_{i\ell}^{(3)} = \sum_{n=P}^{N-1} \hat{\tilde{\mathbf{h}}}_i(n)^{\dagger}\hat{\mathbf{Q}}^{-1}\hat{\tilde{\mathbf{h}}}_\ell(n). \end{cases} \tag{30}$$

$$\begin{aligned}&\left[\mathbf{I}^{-1}(\boldsymbol{\theta})\right]_{\boldsymbol{\theta}_r,\boldsymbol{\theta}_r} \\ &= \operatorname{diag}\left(\left[\sum_{n=P}^{N-1} \tilde{\mathbf{h}}_1^{\dagger}(n)\mathbf{Q}^{-1}\tilde{\mathbf{h}}_1(n)\right]^{-1}\left[\sum_{n=P}^{N-1} \tilde{\mathbf{h}}_1^{\dagger}(n)\mathbf{Q}^{-1}\tilde{\mathbf{h}}_1(n)\right]^{-1}, \ldots, \left[\sum_{n=P}^{N-1} \tilde{\mathbf{h}}_r^{\dagger}(n)\mathbf{Q}^{-1}\tilde{\mathbf{h}}_r(n)\right]^{-1}\left[\sum_{n=P}^{N-1} \tilde{\mathbf{h}}_r^{\dagger}(n)\mathbf{Q}^{-1}\tilde{\mathbf{h}}_r(n)\right]^{-1}\right).\end{aligned} \tag{22}$$

$$\sum_{\ell=1}^{r}\sum_{i=1}^{r} \left[\sum_{n=P}^{N-1} \tilde{\mathbf{x}}_0(n)^{\dagger}\mathbf{Q}^{-1}\tilde{\mathbf{h}}_i(n)\right]\left[\sum_{n=P}^{N-1} \tilde{\mathbf{h}}_i^{\dagger}(n)\mathbf{Q}^{-1}\tilde{\mathbf{h}}_\ell(n)\right]^{-1}\left[\sum_{n=P}^{N-1} \tilde{\mathbf{h}}_\ell(n)^{\dagger}\mathbf{Q}^{-1}\tilde{\mathbf{x}}_0(n)\right] \underset{H_0}{\overset{H_1}{\gtrless}} \xi. \tag{23}$$

TABLE I
COMPLEXITY OF THE SP-RAO DETECTOR

Calculation	Flops
(62)	$O((K+1)(N-P)J^2)$
(63)	$O((K+1)(N-P)J^2P^2)$
(64)	$O((K+1)(N-P)J^2P)$
(24)	$O(J^2(P^3+P^2))$
(25)	$O(J^2P)$
(26)	$O((K+1)NJ^2P^2)+O((N-P)r^2J^3)$

Therefore, the final expression for Λ is given by

$$\Lambda = \sum_{\ell=i} t_{\ell,i} + \sum_{\substack{\ell=1 \\ (\ell<i)}}^{r-1} \sum_{i=\ell+1}^{r} \frac{2\Re(t_i^{(1)})\Re(t_\ell^{(2)})}{\Re(t_{i\ell}^{(3)})} + \sum_{\substack{i=1 \\ (\ell>i)}}^{r-1} \sum_{\ell=i+1}^{r} \frac{2\Re(t_i^{(1)})\Re(t_\ell^{(2)})}{\Re(t_{i\ell}^{(3)})}. \tag{31}$$

Note that the above subspace parametric Rao detector employs a new multi-rank structure that involves pairwise successive spatio-temporal whitening and a cross-correlation process between the test signal and each subspace basis vector. This is different from traditional parametric rank-one signal detection, which performs the whitening and cross-correlation process using only the signal steering vector. Moreover, note also that the proposed subspace parametric detector (31) only requires the estimation of the AR coefficient matrix $\mathbf{A}$ and the $J \times J$ covariance matrix $\mathbf{Q}$, instead of the $NJ \times NJ$ covariance matrix $\mathbf{R}$. Consequently, it is expected that the proposed subspace parametric detector is well suited to training-limited scenarios, where the number of training data is smaller than the system dimension. This will be confirmed by numerical results in Section IV.

We now briefly discuss the complexity of the proposed SP-Rao. Suppose $KN > JP$ for the parametric detection. Table I contains a summary of the number of flops involved in the major steps of the SP-Rao. It can be seen from Table I that the proposed SP-Rao has an overall complexity of $O((K+1)NJ^2P^2) + O((N-P)r^2J^3)$, which mainly comes from the estimation of spatial whitening matrix and the calculation of the test statistics.

B. A Non-Parametric Subspace Detector

After obtaining the adaptive subspace parametric Rao test (31), weconsider the relationship between (31) and non-parametric subspace detectors. In the sequel, we first derive a new detector from (31), which takes a non-parametric form, and then compare the proposed detectors with traditional ones.

By spatial whitening, (26) reduces to

$$\Lambda_2 = \sum_{\ell=1}^{r} \sum_{i=1}^{r} \frac{\left(\sum_{n=P}^{N-1} \hat{\tilde{\mathbf{x}}}_0(n)^\dagger \hat{\tilde{\mathbf{h}}}_i(n)\right)\left(\sum_{n=P}^{N-1} \hat{\tilde{\mathbf{h}}}_\ell(n)^\dagger \hat{\tilde{\mathbf{x}}}_0(n)\right)}{\sum_{n=P}^{N-1} \hat{\tilde{\mathbf{h}}}_i(n)^\dagger \hat{\tilde{\mathbf{h}}}_\ell(n)}, \tag{32}$$

where for notational convenience, we again use $\hat{\tilde{\mathbf{x}}}_0(n)$ and $\hat{\tilde{\mathbf{h}}}_i(n)$ for $i = 1, \ldots, r$ instead of the corresponding whitened vector.

Denote $\mathbf{A}(f)$ as the reciprocal of the frequency response of the AR processing, which is a $J \times J$ matrix function of frequency f. Similarly, denote

$$\mathbf{S}_i(f) = \sum_{n=0}^{N-1} \mathbf{h}_i(n)\exp(-j2\pi fn) \tag{33}$$

as the Fourier transform of the $J \times 1$ spatial vector $\mathbf{h}_i(n)$, and

$$\mathbf{X}(f) = \sum_{n=0}^{N-1} \mathbf{x}_0(n)\exp(-j2\pi fn) \tag{34}$$

as the Fourier transform of the $J \times 1$ spatial vector $\mathbf{x}_0(n)$. Thus, using Parseval's theorem, the (l,i)th term of the double sum in (32) can be written as

$$\frac{\int_{-\frac{1}{2}}^{\frac{1}{2}} \mathbf{S}_i^\dagger(f)\mathbf{A}^T(f)\mathbf{A}^*(f)\mathbf{X}(f)df \int_{-\frac{1}{2}}^{\frac{1}{2}} \mathbf{S}_\ell^\dagger(f)\mathbf{A}^T(f)\mathbf{A}^*(f)\mathbf{X}(f)df}{\int_{-\frac{1}{2}}^{\frac{1}{2}} \mathbf{S}_i^\dagger(f)\mathbf{A}^T(f)\mathbf{A}^*(f)\mathbf{S}_\ell(f)df}. \tag{35}$$

The cross-spectral matrix (CSM) of a multichannel AR process is given by [39]

$$\mathbf{P}(f) = \mathbf{A}^{*-1}(f)\mathbf{A}^{T-1}(f). \tag{36}$$

Substituting (36) into the double sum with the term (35) yields

$$\sum_{\ell=1}^{r}\sum_{i=1}^{r} \frac{\int_{-\frac{1}{2}}^{\frac{1}{2}} \mathbf{S}_i^\dagger(f)\mathbf{P}^{-1}(f)\mathbf{X}(f)df \int_{-\frac{1}{2}}^{\frac{1}{2}} \mathbf{S}_\ell^\dagger(f)\mathbf{P}^{-1}(f)\mathbf{X}(f)df}{\int_{-\frac{1}{2}}^{\frac{1}{2}} \mathbf{S}_i^\dagger(f)\mathbf{P}^{-1}(f)\mathbf{S}_\ell(f)df}. \tag{37}$$

Next, we use the fact that $\mathbf{R}$ can be asymptotically block diagonalized. Here, "asympotic" relates to a large number of temporal blocks, namely, $N \longrightarrow \infty$. Define the multichannel sinusoidal matrix as

$$\mathbf{V}_k = \frac{1}{\sqrt{N}} \begin{bmatrix} \mathbf{I}_J \\ \mathbf{I}_J\exp(j2\pi f_k) \\ \vdots \\ \mathbf{I}_J\exp[j2\pi f_k(N-1)] \end{bmatrix}, \tag{38}$$

where $f_k = k/N$ for $k = 0, \ldots, N-1$, $\mathbf{I}_J$ is the $J \times J$ identity matrix, and the size of $\mathbf{V}_k$ is $JN \times J$. Let

$$\mathbf{V} = [\mathbf{V}_0 \quad \mathbf{V}_1 \quad \cdots \quad \mathbf{V}_{N-1}] \tag{39}$$

and

$$\widetilde{\mathbf{P}}^T = \begin{bmatrix} \mathbf{P}^T(f_0) & \mathbf{0} & \cdots & \mathbf{0} \\ \mathbf{0} & \mathbf{P}^T(f_1) & \cdots & \mathbf{0} \\ \vdots & \vdots & \ddots & \vdots \\ \mathbf{0} & \mathbf{0} & \cdots & \mathbf{P}^T(f_{N-1}) \end{bmatrix}. \tag{40}$$

Note that $\mathbf{V}$ is a unitary matrix. For large N, we have [41]

$$\mathbf{V}^H\mathbf{R}\mathbf{V} = \widetilde{\mathbf{P}}^T. \tag{41}$$

TABLE II
COMPLEXITY OF THE NSD DETECTOR

Calculation	Flops
$\hat{\mathbf{R}}$	$O(KJ^2N^2)$
$\hat{\mathbf{R}}^{-1}$	$O(J^3N^3)$
(45)	$O(KJ^2N^2)+O(J^3N^3)+O(r^2J^3N^3)$

Using (41), we rewrite $\mathbf{h}_i^\dagger\mathbf{R}^{-1}\mathbf{h}_\ell$ as

$$\begin{aligned}\mathbf{h}_i^\dagger\,\mathbf{R}^{-1}\,\mathbf{h}_\ell &= \mathbf{h}_i^\dagger\,\mathbf{V}\,\widetilde{\mathbf{P}}^{-T}\,\mathbf{V}^\dagger\,\mathbf{h}_\ell \\ &= \frac{1}{N}\sum_{n=0}^{N-1}\mathbf{S}_i^\dagger(f_n)\mathbf{P}^{-1}(f_n)\mathbf{S}_\ell(f_n) \\ &= \int_{-\frac{1}{2}}^{\frac{1}{2}}\mathbf{S}_i^\dagger(f)\mathbf{A}^T(f)\mathbf{A}^*(f)\mathbf{S}_\ell(f)df, \qquad (42)\end{aligned}$$

where the second equality is due to the fact that $\mathbf{V}_k^\dagger\mathbf{h}_\ell = \mathbf{S}_\ell(f_k),\ k=0,\ldots,N-1$.

Similarly, we can obtain that

$$\mathbf{h}_\ell^\dagger\mathbf{R}^{-1}\mathbf{x}_0 = \int_{-\frac{1}{2}}^{\frac{1}{2}}\mathbf{S}_\ell^\dagger(f)\mathbf{P}^{-1}(f)\mathbf{X}(f)df. \qquad (43)$$

Substituting (42) and (43) into (37) yields

$$\Lambda_2 = \sum_{i=1}^{r}\sum_{\ell=1}^{r}\mathbf{x}_0^\dagger\mathbf{R}^{-1}\mathbf{h}_i\left(\mathbf{h}_i^\dagger\mathbf{R}^{-1}\mathbf{h}_\ell\right)^{-1}\mathbf{h}_\ell^\dagger\mathbf{R}^{-1}\mathbf{x}_0. \qquad (44)$$

In order to make the detector (44) fully adaptive, we resort to the sample covariance matrix estimation $\hat{\mathbf{R}} = \sum_{k=1}^{K}\mathbf{x}_k\mathbf{x}_k^\dagger$. Thus, replacing the covariance matrix in (44) with $\hat{\mathbf{R}}$ results in

$$\Lambda_2 = \sum_{i=1}^{r}\sum_{\ell=1}^{r}\mathbf{x}_0^\dagger\hat{\mathbf{R}}^{-1}\mathbf{h}_i\left(\mathbf{h}_i^\dagger\hat{\mathbf{R}}^{-1}\mathbf{h}_\ell\right)^{-1}\mathbf{h}_\ell^\dagger\hat{\mathbf{R}}^{-1}\mathbf{x}_0. \qquad (45)$$

Similarly, (45) can be expressed as

$$\begin{aligned}\Lambda_2 &= \sum_{\ell=i}\mathbf{x}_0^\dagger\hat{\mathbf{R}}^{-1}\mathbf{h}_i(\mathbf{h}_i^\dagger\hat{\mathbf{R}}^{-1}\mathbf{h}_\ell)^{-1}\mathbf{h}_\ell^\dagger\hat{\mathbf{R}}^{-1}\mathbf{x}_0 \\ &\quad+\sum_{\substack{\ell=1\\(\ell<i)}}^{r-1}\sum_{i=\ell+1}^{r}\frac{2\Re(\mathbf{x}_0^\dagger\hat{\mathbf{R}}^{-1}\mathbf{h}_i)\Re(\mathbf{h}_\ell^\dagger\hat{\mathbf{R}}^{-1}\mathbf{x}_0)}{\Re(\mathbf{h}_i^\dagger\hat{\mathbf{R}}^{-1}\mathbf{h}_\ell)} \\ &\quad+\sum_{\substack{i=1\\(\ell>i)}}^{r-1}\sum_{\ell=i+1}^{r}\frac{2\Re(\mathbf{x}_0^\dagger\hat{\mathbf{R}}^{-1}\mathbf{h}_i)\Re(\mathbf{h}_\ell^\dagger\hat{\mathbf{R}}^{-1}\mathbf{x}_0)}{\Re(\mathbf{h}_i^\dagger\hat{\mathbf{R}}^{-1}\mathbf{h}_\ell)}. \qquad (46)\end{aligned}$$

Finally, a short analysis on the complexity of the proposed NSD is presented. Suppose $N > P^2$. Table II contains a summary of the number of flops involved in the major steps of the NSD. It can be seen from Table II that the proposed NSD has an overall complexity of $O(KJ^2N^2)+O(J^3N^3)+O(r^2J^3N^3)$, which mainly comes from the estimation of the sample covariance matrix matrix and the calculation of the the test statistics. It is higher than the complexity of the SP-Rao.

TABLE III
SUMMARY OF TEST STATISTICS

Detector	Test Statistic
SP-Rao	$\sum_{\ell=1}^{r}\sum_{i=1}^{r}\frac{\left(\sum_{n=P}^{N-1}\hat{\tilde{\mathbf{x}}}_0(n)^\dagger\hat{\mathbf{Q}}^{-1}\hat{\tilde{\mathbf{h}}}_i(n)\right)\left(\sum_{n=P}^{N-1}\hat{\tilde{\mathbf{h}}}_\ell(n)^\dagger\hat{\mathbf{Q}}^{-1}\hat{\tilde{\mathbf{x}}}_0(n)\right)}{\sum_{n=P}^{N-1}\hat{\tilde{\mathbf{h}}}_i^\dagger(n)\hat{\mathbf{Q}}^{-1}\hat{\tilde{\mathbf{h}}}_\ell(n)}$
NSD	$\sum_{i=1}^{r}\sum_{\ell=1}^{r}\mathbf{x}_0^\dagger\hat{\mathbf{R}}^{-1}\mathbf{h}_i\left(\mathbf{h}_i^\dagger\hat{\mathbf{R}}^{-1}\mathbf{h}_\ell\right)^{-1}\mathbf{h}_\ell^\dagger\hat{\mathbf{R}}^{-1}\mathbf{x}_0$
rank-one PRao [30]	$\frac{\left\lvert\sum_{n=P}^{N-1}\hat{\tilde{\mathbf{x}}}_0(n)^\dagger\hat{\mathbf{Q}}^{-1}\hat{\tilde{\mathbf{h}}}(n)\right\rvert^2}{\sum_{n=P}^{N-1}\hat{\tilde{\mathbf{h}}}^\dagger(n)\hat{\mathbf{Q}}^{-1}\hat{\tilde{\mathbf{h}}}(n)}$
Rao [11]	$\frac{\tilde{\mathbf{x}}_0^\dagger\mathbf{P}_{\tilde{\mathbf{H}}}\tilde{\mathbf{x}}_0}{(1+\tilde{\mathbf{x}}_0^\dagger\tilde{\mathbf{x}}_0)(1+\tilde{\mathbf{x}}_0^\dagger\mathbf{P}_{\tilde{\mathbf{H}}}^\perp\tilde{\mathbf{x}}_0)}$
GLRT [10]	$\frac{\mathbf{x}_0^\dagger\hat{\mathbf{R}}^{-1}\mathbf{H}(\mathbf{H}^\dagger\hat{\mathbf{R}}^{-1}\mathbf{H})^{-1}\mathbf{H}^\dagger\hat{\mathbf{R}}^{-1}\mathbf{x}_0}{1+\mathbf{x}_0^\dagger\hat{\mathbf{R}}^{-1}\mathbf{x}_0}$
AMF [6]	$\mathbf{x}_0^\dagger\hat{\mathbf{R}}^{-1}\mathbf{H}(\mathbf{H}^\dagger\hat{\mathbf{R}}^{-1}\mathbf{H})^{-1}\mathbf{H}^\dagger\hat{\mathbf{R}}^{-1}\mathbf{x}_0$
rank-one ACE [2]	$\mathbf{x}_0^\dagger\hat{\mathbf{R}}^{-1}\mathbf{h}(\mathbf{h}^\dagger\hat{\mathbf{R}}^{-1}\mathbf{h})^{-1}\mathbf{h}^\dagger\hat{\mathbf{R}}^{-1}\mathbf{x}_0$

C. Summary of Relevant Tests

For comparison purposes, we compare the proposed detectors with the GLRT [10] , the AMF [6], the Rao [11], the rank-one PRao [30], and the rank-one ACE [2]. Their test statistics are given in Table III, where

$$\tilde{\mathbf{H}} = \hat{\mathbf{R}}^{-1/2}\mathbf{H}, \qquad (47)$$

$$\tilde{\mathbf{x}}_0 = \hat{\mathbf{R}}^{-1/2}\mathbf{x}_0, \qquad (48)$$

$$\mathbf{P}_{\tilde{\mathbf{H}}} = \tilde{\mathbf{H}}(\tilde{\mathbf{H}}^\dagger\tilde{\mathbf{H}})^{-1}\tilde{\mathbf{H}}^\dagger, \qquad (49)$$

$$\mathbf{P}_{\tilde{\mathbf{H}}}^\perp = \mathbf{I}-\tilde{\mathbf{H}}(\tilde{\mathbf{H}}^\dagger\tilde{\mathbf{H}})^{-1}\tilde{\mathbf{H}}^\dagger. \qquad (50)$$

Note that the conventional detectors such as the rank-one ACE and the rank-one PRao are all designed for rank-one signal detection. Thus, they cannot be applied to the multi-rank subspace detection problem with $r > 1$ in (5) to account for uncertainties of the signal steering vector. Unlike conventional detectors, the SP-Rao has a new multi-rank structure, which helps improve its performance when the number of training data is limited. This prediction will be confirmed by simulation results in Section IV. It is worth noting that conventional non-parametric subspace detectors such as the GLRT, the Rao and the AMF (as a special case, the AMF reduces to the rank-one ACE for $r = 1$), perform matched filtering using the entire subspace matrix. In contrast, our non-parametric NSD performs pairwise whitening and cross-correlation using individual subspace basis vector. Additionally, for the special case $r = 1$, the rank-one PRao reduces to the rank-one Rao [41] and the NSD reduces to the rank-one ACE.

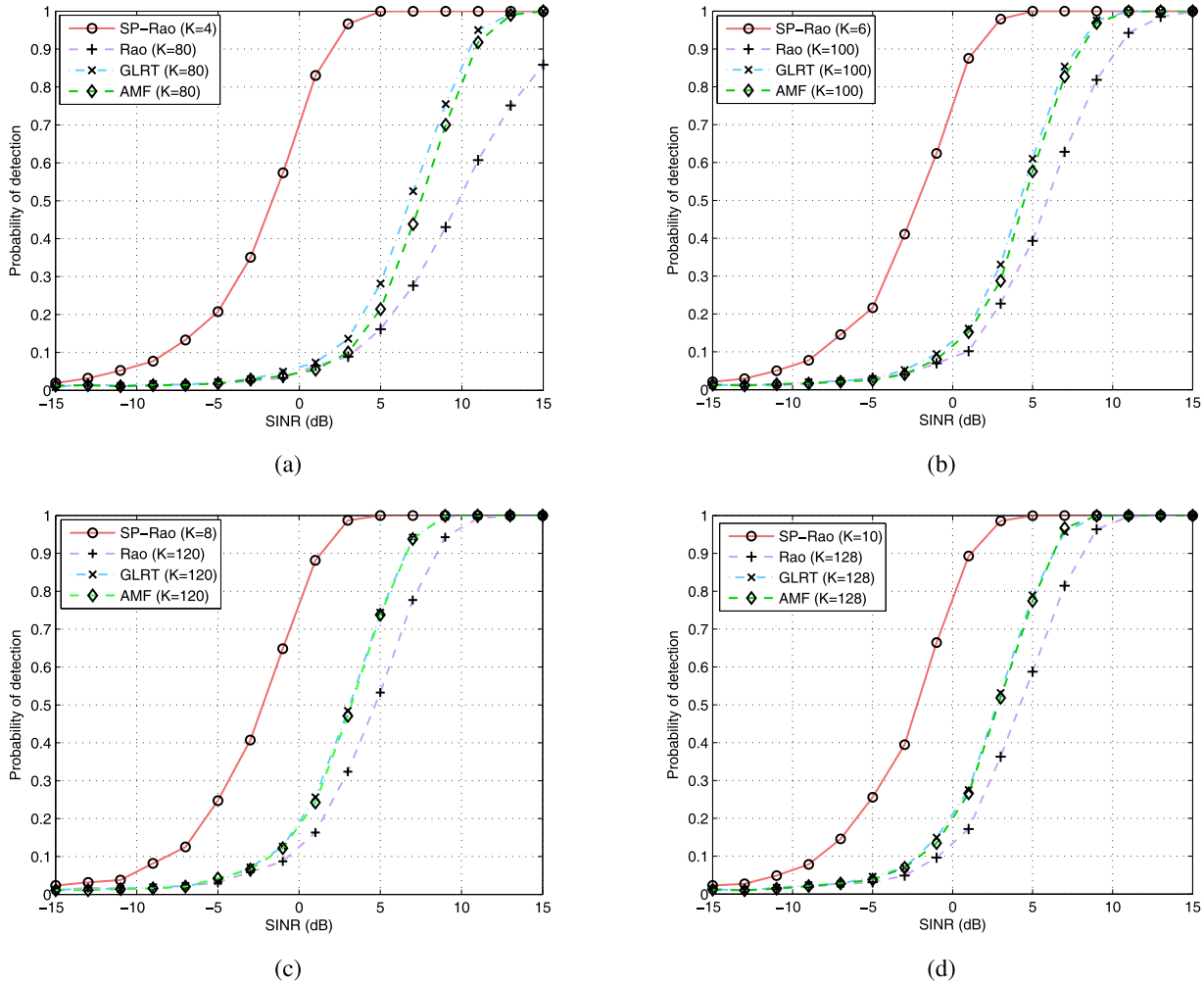

Fig. 1. Probability of detection versus SINR with different number of training data.

IV. Numerical Results

In this section, numerical examples are provided to assess the performance of the proposed detectors. For comparison purposes, we compare the proposed SP-Rao with the GLRT, the AMF, the Rao, and the rank-one PRao, and compare the proposed NSD with the rank-one ACE. The disturbance signal is generated as a multichannel AR(2) process with AR coefficient $\mathbf{A}$ and a spatial covariance matrix $\mathbf{Q}$. These parameters are set to ensure that the AR process is stable and $\mathbf{Q}$ is a valid covariance matrix, but otherwise are randomly selected. As to $\mathbf{R}$, it is uniquely determined once $\mathbf{A}$ and $\mathbf{Q}$ are selected. To decrease the computational load, the probability of false alarm P_{fa} is chosen to be 10^{-2}, and the number of independent trials is $100/P_{fa}$. The signal vectors correspond to a uniform equispaced linear array with $J = 4$ antenna elements and $N = 16$ temporal pulses. The signal subspace $\langle \mathbf{H} \rangle$ is spanned by a $r = 3$ matrix $\mathbf{H}$, where the column vector $\mathbf{h}_i$ of subspace $\mathbf{H}$ is given by

$$\mathbf{h}_i = \mathbf{h}_{it}(f_{di}) \otimes \mathbf{h}_{is}(f_{si}), \tag{51}$$

where $\mathbf{h}_{it}(f_{di})$ denotes the temporal steering vector with Doppler frequency f_{di}:

$$\mathbf{h}_{it}(f_{di}) = \frac{1}{N}[1, \mathrm{e}^{-j2\pi f_{di}}, \ldots, \mathrm{e}^{-j2\pi f_{di}(N-1)}]^T, \tag{52}$$

and $\mathbf{h}_{is}(f_{si})$ denotes the spatial steering vector with spatial frequency f_{si}:

$$\mathbf{h}_{is}(f_{si}) = \frac{1}{N}[1, \mathrm{e}^{-j2\pi f_{si}}, \cdots, \mathrm{e}^{-j2\pi f_{si}(J-1)}]^T. \tag{53}$$

The Doppler frequency and spatial frequency are assumed to be identical. For the signal subspace, there is a mismatch of Δ with respect to the nominal Doppler/spatial frequency $f_0 = 0.1$. Unless otherwise stated, we set $\Delta = 0.01$. The spatial/Doppler frequencies for the rank-3 matrix $\mathbf{H}$ are given by $[f_0 - \Delta, f_0, f_0 + \Delta]$.

The signal-to-interference-plus-noise ratio (SINR) is defined as

$$\mathrm{SINR} = \boldsymbol{\alpha}^\dagger \mathbf{H}^\dagger \mathbf{R}^{-1} \mathbf{H} \boldsymbol{\alpha}. \tag{54}$$

Fig. 1 shows the probability of detection versus SINR for the proposed SP-Rao, where $K = 4$, 6, 8, and 10, respectively. The number of training data for the conventional subspace detectors (i.e., the GLRT, the AMF and the Rao) is $K = 80$, 100, 120, 128, respectively, since it needs to be more than the system dimension to avoid the singularity of the sample covariance matrix [15]. It is seen in Fig. 1 that the proposed SP-Rao, using much fewer training samples, significantly outperforms the other detectors. This is as expected, since the SP-Rao involves

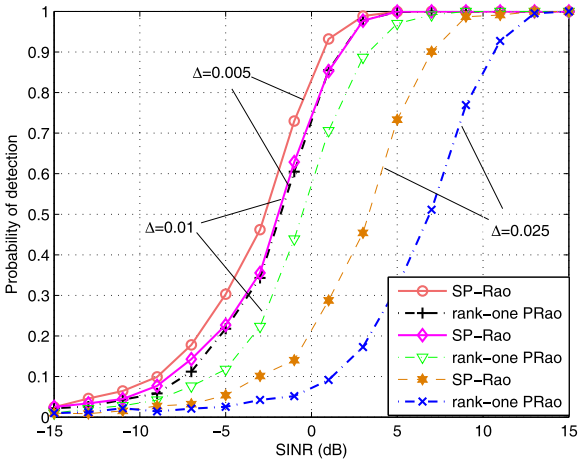

Fig. 2. Probability of detection versus SINR with different amount of uncertainty.

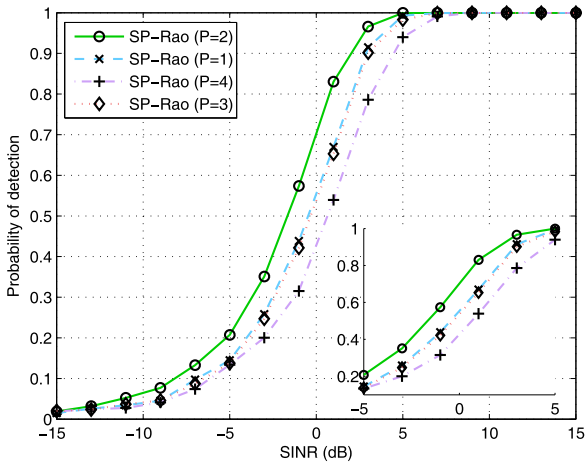

Fig. 3. Probability of detection versus SINR with model order mismatch.

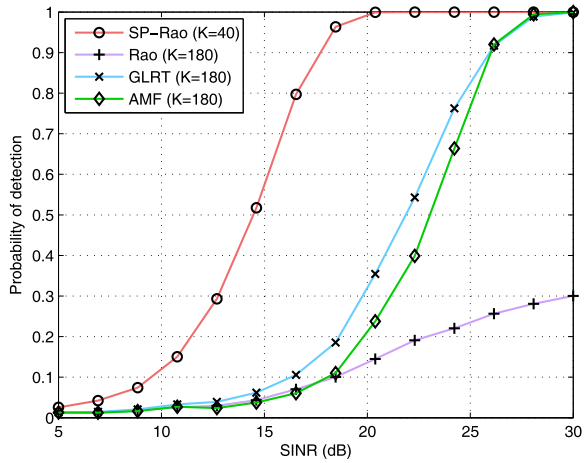

Fig. 4. Probability of detection versus SINR with non-AR disturbance.

a smaller dimension estimation of the AR parameters instead of a rather large spatial-temporal dimension estimation of the covariance matrix. It is also observed that increasing the sample size can produce a detection gain to all these detectors. But the performance the SP-Rao is still the best.

We now examine the effect of different amount of uncertainty on the detection performance, where the mismatch Δ is given by 0.005, 0.01 and 0.025, respectively. For comparison purposes, the results of the proposed SP-Rao and the traditional rank-one P-Rao with the same sample size $K = 2$ are presented. Note that the simulation results for the conventional subspace detectors are unavailable for this case, since they are not functional for $K < NJ$. As shown in Fig. 2, the detection performance improves with smaller uncertainty. On the other hand, it is seen that the proposed SP-Rao performs notably better than the rank-one P-Rao, although both are provided with the the same sample support. It implies that SP-Rao can not only improve the detection performance in training-limited scenarios, but also produce a detection gain in the case of signal mismatch.

The above results assume that the disturbance is an exact multichannel AR process with a known model order. However, model mismatch often occurs in practice. For example, the estimation procedure of the AR model order for the multichannel AR process may experience a small estimation error. In addition, the disturbance in real world may not be an exact AR process. Thus, we evaluate the detection performance of the proposed SP-Rao when these assumptions are not met. First, we consider the case when the disturbance is an AR Process, but estimation error for the model order exists. Fig. 3 illustrates the performance of the proposed SP-Rao when the model order is underestimated ($P = 1$) and overestimated ($P = 3,\ 4$), whereas the true order is $P = 2$. As shown in Fig. 3, the order mismatch causes some performance degradation. However, the degradation is not significant. It is also observed that the larger the gap between the true and the estimated orders, the larger the performance degradation. Second, we consider the case when the disturbance is generated from a physical clutter model described in [15], rather than a multichannel AR process. Specifically, a uniform linear array with 11 elements is used and the number of pulses is 16. The platform velocity is 120 m/s and the wavelength is 0.32 m. The clutter-to-noise ratio is 60 dB. The pulse repetition frequency is 1500 Hz. The number of training samples for the proposed SP-Rao and for the traditional detectors is 40 and 180, respectively. The results are depicted in Fig. 4. As shown in Fig. 4, the performance of the traditional detectors is still worse than the proposed SP-Rao in this scenario. It indicates that the performance of the SP-Rao appears not to be sensitive to the model mismatch.

We now examine the performance of the proposed NSD with different sizes of training data, where $K = 80$, 100, and 120, respectively. Note that the number of training data for the NSD should be no less than the system dimension [15], since it is a non-parametric detector. As a benchmark, the proposed SP-Rao with $K = 4$ is also provided. The results of the probability of detection versus the SNR are depicted in Fig. 5. It is seen that the detection probability of the proposed NSD increases as the size of training data becomes large. As K increase, the performance

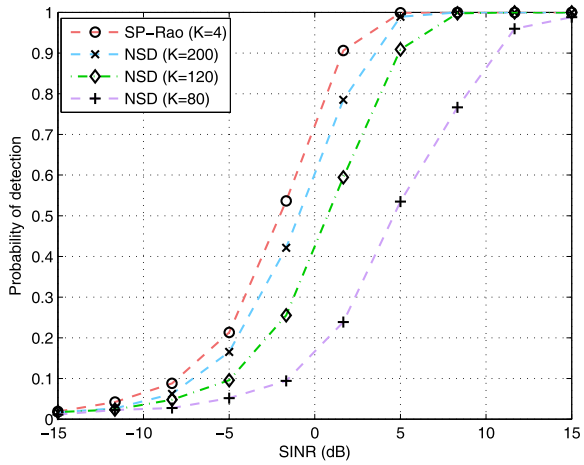

Fig. 5. Probability of detection versus SINR for the NSD.

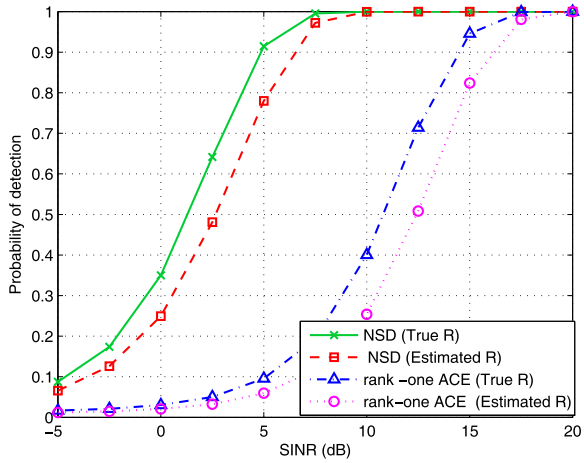

Fig. 6. Comparision of the NSD with the ACE.

of the NSD is nearly identical to that of the SP-Rao; hence highlighting the benefits of large training support.

It is also interesting to compare the proposed NSD approach with the traditional rank-one ACE, since the NSD reduces to the rank-one ACE for $r = 1$. However, it has to be emphasized here that for $r > 1$ the rank-one ACE cannot be directly used in the multi-rank subspace signal detection problem. Thus, its steering vector is randomly selected from the $r = 3$ subspace columns of the subspace. The probability of detection versus SNR for $N = 16, K = 64, r = 3$ are presented in Fig. 6, where both the true and the estimated covariance matrices are considered. As seen in Fig. 6, the proposed NSD shows notably better detection performance than the rank-one ACE. This is expected, as the rank-one ACE is designed only for rank-one signal.

V. Conclusion

This paper considered a subspace signal detection problem with spatially and temporally colored disturbance for STAP applications, where the target signal belongs to a known subspace, but with unknown coordinates. We presented a subspace parametric Rao detector, referred to as the SP-Rao, which involves a new multi-rank structure with a pairwise successive spatio-temporal whitening and cross-correlation between the observed signal and each subspace basis vector. In addition, a non-parametric subspace detector, referred to as the NSD, was derived based on a frequency-domain representation of the SP-Rao test statistic. The NSD involves pairwise whitening and cross-correlation between the test signal and each subspace basis vector rather than the full subspace matrix employed by conventional detectors. Interestingly, the SP-Rao and the NSD reduced respectively to the conventional rank-one PRao and rank-one ACE when the target is a rank-one signal. Simulation results demonstrated that the proposed detectors yielded enhanced performance in training-limited scenarios.

Appendix A
Derivation of the Inverse of the Fisher Information Matrix

As the signal parameter $\boldsymbol{\theta}_r$ is contained only in the mean of $\mathbf{x}_0$ and the noise parameter $\boldsymbol{\theta}_s$ only in the covariance matrix of $\mathbf{R}$, we have $\mathbf{I}_{\boldsymbol{\theta}_r,\boldsymbol{\theta}_s}(\boldsymbol{\theta}) = 0$ according to [41, Eq.(3.31)]. Thus, it follows from (13) that

$$\left[\mathbf{I}^{-1}(\boldsymbol{\theta})\right]_{\boldsymbol{\theta}_r,\boldsymbol{\theta}_r} = \mathbf{I}^{-1}_{\boldsymbol{\theta}_r,\boldsymbol{\theta}_r}(\boldsymbol{\theta}). \tag{55}$$

Now we compute $\mathbf{I}^{-1}_{\boldsymbol{\theta}_r,\boldsymbol{\theta}_r}(\boldsymbol{\theta})$ as follows. First, $\mathbf{I}_{\boldsymbol{\theta}_r,\boldsymbol{\theta}_r}(\boldsymbol{\theta})$ is a $J \times J$ matrix with the (i,ℓ)th element

$$\left\{\mathbf{I}_{\boldsymbol{\theta}_r,\boldsymbol{\theta}_r}(\boldsymbol{\theta})\right\}_{i,\ell} = -E\left[\frac{\partial^2 \ln f}{\partial \boldsymbol{\theta}_{r,i}\partial \boldsymbol{\theta}_{r,\ell}}\right], i,l = 1,\ldots,r, \tag{56}$$

where $\boldsymbol{\theta}_{r,i}$ and $\boldsymbol{\theta}_{r,\ell}$ are the ith and ℓth elements of $\boldsymbol{\theta}$, respectively.

The second partial derivative of the log likelihood function w.r.t. $\boldsymbol{\theta}_r$ is

$$\begin{cases} \frac{\partial^2 \ln f}{\partial \alpha_{R,i}\partial \alpha_{R,\ell}} = -2\sum_{n=P}^{N-1}\tilde{\mathbf{h}}_i^{\dagger}(n)\mathbf{Q}^{-1}\tilde{\mathbf{h}}_{\ell}(n) \\ \frac{\partial^2 \ln f}{\partial \alpha_{I,i}\partial \alpha_{I,\ell}} = -2\sum_{n=P}^{N-1}\tilde{\mathbf{h}}_i^{\dagger}(n)\mathbf{Q}^{-1}\tilde{\mathbf{h}}_{\ell}(n) \\ \frac{\partial^2 \ln f}{\partial \alpha_{R,i}\partial \alpha_{I,\ell}} = \frac{\partial^2 \ln f}{\partial \alpha_{I,i}\partial \alpha_{R,\ell}} = 0. \end{cases} \tag{57}$$

According to (56) and (57), $\mathbf{I}_{\boldsymbol{\theta}_r,\boldsymbol{\theta}_r}(\boldsymbol{\theta})$ is given by

$$\mathbf{I}_{\boldsymbol{\theta}_r,\boldsymbol{\theta}_r}(\boldsymbol{\theta}) = 2\,\mathrm{diag}\left[\sum_{n=P}^{N-1}\tilde{\mathbf{h}}_1^{\dagger}(n)\mathbf{Q}^{-1}\tilde{\mathbf{h}}_1(n), \sum_{n=P}^{N-1}\tilde{\mathbf{h}}_1^{\dagger}(n)\mathbf{Q}^{-1}\tilde{\mathbf{h}}_1(n), \ldots, \sum_{n=P}^{N-1}\tilde{\mathbf{h}}_r^{\dagger}(n)\mathbf{Q}^{-1}\tilde{\mathbf{h}}_r(n), \sum_{n=P}^{N-1}\tilde{\mathbf{h}}_r^{\dagger}(n)\mathbf{Q}^{-1}\tilde{\mathbf{h}}_r(n)\right]. \tag{58}$$

Appendix B
ML Parameter Estimate Under H_0

From (14), the joint PDF under H_0 is $f(\boldsymbol{\theta})$ with $\boldsymbol{\alpha} = 0$. By taking the derivative of the log likelihood $\ln f(\boldsymbol{\theta})$ with $\boldsymbol{\alpha} = 0$ w.r.t. $\mathbf{Q}$ and equating it to zero yields the ML estimate of $\mathbf{Q}$ as

$$\hat{\mathbf{Q}} = \mathbf{T}(\mathbf{A}) = \sum_{n=P}^{N-1}\boldsymbol{\varepsilon}_0(n)\boldsymbol{\varepsilon}_0(n)^{\dagger} + \sum_{k=1}^{K}\sum_{n=P}^{N-1}\boldsymbol{\varepsilon}_k(n)\boldsymbol{\varepsilon}_k(n)^{\dagger}. \tag{59}$$

Substituting $\hat{\mathbf{Q}}$ into $\ln f(\boldsymbol{\theta})$ under H_0 yields

$$f(\mathbf{A},\hat{\mathbf{Q}}) = \left\{ \frac{(\mathrm{e}\pi)^{-J}}{\left|\mathbf{T}(\mathbf{A})\right|} \right\}^{(K+1)(N-P)} \tag{60}$$

Thus, the ML estimate of $\mathbf{A}$ is obtained by minimizing $|\mathbf{T}(\mathbf{A})|$. As $\mathbf{T}(\mathbf{A})$ can be rewritten as

$$\mathbf{T}(\mathbf{A}) = \frac{\hat{\mathbf{R}}_{xx} + \mathbf{A}^{\dagger}\hat{\mathbf{R}}_{yx} + \mathbf{A}^{\dagger}\hat{\mathbf{R}}_{yy}\mathbf{A}}{(K+1)(N-P)}, \tag{61}$$

where

$$\hat{\mathbf{R}}_{xx} = \sum_{n=P}^{N-1} \mathbf{x}_0(n)\mathbf{x}_0(n)^{\dagger} + \sum_{k=1}^{K}\sum_{n=P}^{N-1} \mathbf{x}_k(n)\mathbf{x}_k(n)^{\dagger}, \tag{62}$$

$$\hat{\mathbf{R}}_{yy} = \sum_{n=P}^{N-1} \mathbf{y}_0(n)\mathbf{y}_0(n)^{\dagger} + \sum_{k=1}^{K}\sum_{n=P}^{N-1} \mathbf{y}_k(n)\mathbf{y}_k(n)^{\dagger}, \tag{63}$$

$$\hat{\mathbf{R}}_{yx} = \sum_{n=P}^{N-1} \mathbf{y}_0(n)\mathbf{x}_0(n)^{\dagger} + \sum_{k=1}^{K}\sum_{n=P}^{N-1} \mathbf{y}_k(n)\mathbf{x}_k(n)^{\dagger}, \tag{64}$$

with

$$\mathbf{y}_k(n) = \left[\mathbf{y}_k^T(n-1), \cdots, \mathbf{y}_k^T(n-P)\right]^T. \tag{65}$$

It can be shown that [30]

$$\mathbf{T}(\mathbf{A}) \geq \mathbf{T}(\hat{\mathbf{A}}), \tag{66}$$

where

$$\hat{\mathbf{A}} = -\hat{\mathbf{R}}_{yx}\hat{\mathbf{R}}_{yy}^{-1}. \tag{67}$$

Therefore, the ML estimate of $\mathbf{Q}$ is given by

$$\hat{\mathbf{Q}} = \frac{\hat{\mathbf{R}}_{xx} - \hat{\mathbf{R}}_{yx}^{\dagger}\hat{\mathbf{R}}_{yy}^{-1}\hat{\mathbf{R}}_{yx}}{(K+1)(N-P)}. \tag{68}$$

REFERENCES

[1] E. J. Kelly, "An adaptive detection algorithm," *IEEE Trans. Aerosp. Electron. Syst.*, vol. 22, no. 1, pp. 115–127, Mar. 1986.

[2] A. De Maio, and M. Greco, *Modern Radar Detection Theory*. Stevenage, U.K.: Inst. Eng. Technol., 2015.

[3] A. De Maio and D. Orlando, "Feature article: A survey on two-stage decision schemes for point-like targets in Gaussian interference," *IEEE Aerosp. Electron. Syst. Mag.*, vol. 31, no. 4, pp. 20–29, Apr. 2016.

[4] A. De Maio, "Robust adaptive radar detection in the presence of steering vector mismatches," *IEEE Trans. Aerosp. Electron. Syst.*, vol. 41, no. 4, pp. 1322–1337, Oct. 2005.

[5] F. Bandiera, D. Orlando, and G. Ricci, *Advanced Radar Detection Schemes Under Mismatched Signal Models*. London, U.K.: Morgan & Claypool, 2009.

[6] A. De Maio and G. Ricci, "A polarimetric adaptive matched filter," *Signal Process.*, vol. 81, no. 12, pp. 2583–2589, Dec. 2001.

[7] X. Wang and H. V. Poor, "Blind multiuser detection: A subspace approach," *IEEE Trans. Inf. Theory*, vol. 44, no. 2, pp. 677–690, Mar. 1998.

[8] J. J. Fuchs, "Multipath time-delay detection and estimation," *IEEE Trans. Signal Process.*, vol. 47, no. 1, pp. 237–243, Jan. 1999.

[9] R. S. Raghavan, N. Pulsone, and D. J. McLaughlin, "Performance of the GLRT for adaptive vector subspace detection," *IEEE Trans. Aerosp. Electron. Syst.*, vol. 32, no. 4, pp. 1473–1487, Oct. 1996.

[10] H. R. Park, J. Li, and H. Wang, "Polarization-space-time domain generalized likelihood ratio detection of radar targets," *Signal Process.*, vol. 41, no. 2, pp. 153–164, Jan. 1995.

[11] J. Liu, W. Liu, B. Chen, H. Liu, H. Li, and C. Hao, "Modified Rao test for multichannel adaptive signal detection," *IEEE Trans. Signal Process.*, vol. 64, no. 3, pp. 714–725, Feb. 2016.

[12] A. De Maio and D. Orlando, "Adaptive radar detection of a subspace signal embedded in subspace structured plus Gaussian interference via invariance," *IEEE Trans. Signal Process.*, vol. 64, no. 8, pp. 2156–2167, Apr. 2016.

[13] F. Bandiera, O. Besson, G. Ricci, and L. L. Scharf, "GLRT based direction detectors in homogeneous noise and subspace interference," *IEEE Trans. Signal Process.*, vol. 55, no. 6, pp. 2386–2394, Jun. 2007.

[14] F. Bandiera, D. Orlando, and G. Ricci, "A subspace-based adaptive sidelobe blanker," *IEEE Trans. Signal Process.*, vol. 56, no. 9, pp. 4141–4151, Sep. 2008.

[15] J. Ward, "Space-time adaptive processing for airborne radar," MIT Lincoln Laboratory, Lexington, MA, USA, Tech. Rep. 1015, Dec. 1994.

[16] A. Aubry, A. De Maio, A. Farina, and M. Wicks, "Knowledge-aided (potentially cognitive) transmit signal and receive filter design in signal-dependent clutter," *IEEE Trans. Aerosp. Electron. Syst.*, vol. 49, no. 1, pp. 93–117, Jan. 2013.

[17] F. Bandiera, O. Besson, and G. Ricci, "Adaptive detection of distributed targets in compound-Gaussian noise without secondary data: A Bayesian approach," *IEEE Trans. Signal Process.*, vol. 59, no. 12, pp. 5698–5708, Dec. 2011.

[18] F. Bandiera, O. Besson, A. Coluccia, and G. Ricci, "ABORT-like detectors: A Bayesian approach," *IEEE Trans. Signal Process.*, vol. 63, no. 19, pp. 5274–5284, Oct. 2015.

[19] A. De Maio, A. Farina, and G. Foglia, "Knowledge-aided Bayesian radar detectors & their application to live data," *IEEE Trans. Aerosp. Electron. Syst.*, vol. 46, no. 1, pp. 170–183, Jan. 2010.

[20] R. Nitzberg, "Application of maximum likelihood estimation of persymmetric covariance matrices to adaptive processing," *IEEE Trans. Aerosp. Electron. Syst.*, vol. 16, no. 1, pp. 124–127, Jan. 1980.

[21] G. Pailloux, P. Forster, J.-P. Ovarlez, and F. Pascal, "Persymmetric adaptive radar detectors," *IEEE Trans. Aerosp. Electron. Syst.*, vol. 47, no. 4, pp. 2376–2390, Oct. 2011.

[22] Y. Gao, G. Liao, S. Zhu, X. Zhang, and D. Yang, "Persymmetric adaptive detectors in homogeneous and partially homogeneous environments," *IEEE Trans. Signal Process.*, vol. 62, no. 2, pp. 331–342, Jan. 2014.

[23] A. De Maio and D. Orlando, "An invariant approach to adaptive radar detection under covariance persymmetry," *IEEE Trans. Signal Process.*, vol. 63, no. 5, pp. 1297–1309, Mar. 2015.

[24] J. Liu, W. Liu, H. Liu, and X. Xia, "Average SINR calculation of a persymmetric sample matrix inversion beamformer," *IEEE Trans. Signal Process.*, vol. 64, no. 8, pp. 2135–2145, Apr. 2016.

[25] G. Foglia, C. Hao, and A. Farina, "Adaptive detection in partially homogeneous clutter with symmetric spectrum," *IEEE Trans. Aerosp. Electron. Syst.*, vol. 53, no. 4, pp. 2110–2119, Aug. 2017.

[26] C. Hao, D. Orlando, G. Foglia, and G. Giunta, "Knowledge-based adaptive detection: Joint exploitation of clutter and system symmetry properties," *IEEE Signal Process. Lett.*, vol. 23, no. 10, pp. 1489–1493, Oct. 2016.

[27] A. De Maio, D. Orlando, C. Hao, and G. Folia, "Adaptive detection of point-like targets in spectrally symmetric interference," *IEEE Trans. Signal Process.*, vol. 64, no. 12, pp. 3207–3220, Jun. 2016.

[28] M. Rangaswamy and J. H. Michels, "A parametric multichannel detection algorithm for correlated non-Gaussian random processes," in *Proc. IEEE Nat. Radar Conf.*, Syracuse, NY, USA, May 1997, pp. 349–354.

[29] J. R. Román, M. Rangaswamy, D. W. Davis, Q. Zhang, B. Himed, and J. H. Michels, "Parametric adaptive matched filter for airborne radar applications," *IEEE Trans. Aerosp. Electron. Syst.*, vol. 36, no. 2, pp. 677–692, Apr. 2000.

[30] K. J. Sohn, H. Li, and B. Himed, "Parametric Rao test for multichannel adaptive signal detection," *IEEE Trans. Aerosp. Electron. Syst.*, vol. 43, no. 3, pp. 920–933, Jul. 2007.

[31] K. J. Sohn, H. Li, and B. Himed, "Parametric GLRT test for multichannel adaptive signal detection," *IEEE Trans. Signal Process.*, vol. 55, no. 11, pp. 5351–5360, Nov. 2007.

[32] P. Wang, H. Li, and B. Himed, "A new parametric GLRT for multichannel adaptive signal detection," *IEEE Trans. Signal Process.*, vol. 58, no. 1, pp. 317–325, Jan. 2010.

[33] Y. I. Abramovich, N. K. Spencer, and D. E. Turley, "Time-varying autoregressive (TVAR) models for multiple radar observations," *IEEE Trans. Signal Process.*, vol. 55, no. 4, pp. 1298–1311, Apr. 2007.

[34] P. Wang, H. Li, and B. Himed, "A parametric moving target detector for distributed MIMO radar in non-homogeneous environment," *IEEE Trans. Signal Process.*, vol. 61, no. 9, pp. 2282–2294, May 2013.

[35] A. L. Swindlehurst and P. Stoica, "Maximum likelihood methods in radar array signal processing," *Proc. IEEE*, vol. 86, no. 2, pp. 421–441, Feb. 1998.

[36] J. B. Billingsley, A. Farina, F. Gini, M. V. Greco, and L. Verrazzani, "Statistical analyses of measured radar ground clutter data," *IEEE Trans. Aerosp. Electron. Syst.*, vol. 35, no. 2, pp. 579–593, Apr. 1999.
[37] M. Greco, F. Bordoni, and F. Gini, "X-band sea-clutter nonstationarity: Influence of long waves," *IEEE J. Ocean. Eng.*, vol. 29, no. 2, pp. 269–283, Apr. 2004.
[38] J. H. Michels, B. Himed, and M. Rangaswamy, "Robust STAP detection in a dense signal airborne radar environment," *Signal Process.*, vol. 84, pp. 1625–1636, 2004.
[39] S. M. Kay, *Modern Spectral Estimation: Theory and Application*. Englewood Cliffs, NJ, USA: Prentice-Hall, 1988.
[40] K. J. Sohn, H. Li, and B. Himed, "Parametric Rao test for multichannel adaptive signal detection," *IEEE Trans. Aerosp. Electron. Syst.*, vol. 43, no. 3, pp. 920–933, Jul. 2007.
[41] S. M. Kay, *Fundamentals of Statistical Signal Processing: Detection Theory*, vol. II. Englewood Cliffs, NJ, USA: Prentice-Hall, 1993.

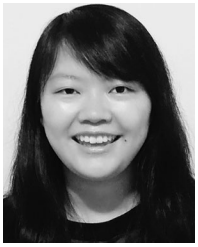

Yongchan Gao (M'16) received the B.S. and Ph.D degrees in electronic engineering from Xidian University, China, in 2009 and 2015, respectively.

From February 2016 to January 2017, she was a Postdoctoral Research Associate with the Department of Electrical and Computer Engineering, Stevens Institute of Technology, Hoboken, NJ, USA. In March 2017, she joined the Department of Electronic Engineering, Xidian University, where she is currently an Associate Professor. Her research interests include adaptive target detection, multistatic radar, passive sensing, and waveform design and diversity.

Hongbin Li (M'99–SM'08) received the B.S. and M.S. degrees from the University of Electronic Science and Technology of China, Chengdu, China, in 1991 and 1994, respectively, and the Ph.D. degree from the University of Florida, Gainesville, FL, USA, in 1999, all in electrical engineering.

From July 1996 to May 1999, he was a Research Assistant with the Department of Electrical and Computer Engineering, University of Florida. Since July 1999, he has been with the Department of Electrical and Computer Engineering, Stevens Institute of Technology, Hoboken, NJ, USA, where he became a Professor in 2010. He was a Summer Visiting Faculty Member with the Air Force Research Laboratory in the summers of 2003, 2004, and 2009. His general research interests include statistical signal processing, wireless communications, and radars.

Dr. Li has been a member of the IEEE SPS Signal Processing Theory and Methods Technical Committee (TC) and the IEEE SPS Sensor Array and Multichannel TC, an Associate Editor for *Signal Processing* (Elsevier), the IEEE TRANSACTIONS ON SIGNAL PROCESSING, the IEEE SIGNAL PROCESSING LETTERS, and the IEEE TRANSACTIONS ON WIRELESS COMMUNICATIONS, as well as a Guest Editor for the IEEE JOURNAL OF SELECTED TOPICS IN SIGNAL PROCESSING and *EURASIP Journal on Applied Signal Processing*. He is a member of the Tau Beta Pi and Phi Kappa Phi societies. He has been involved in various conference organization activities, including serving as a General Co-Chair for the 7th IEEE Sensor Array and Multichannel Signal Processing Workshop, Hoboken, NJ, USA, Jun. 17–20, 2012. He received the IEEE Jack Neubauer Memorial Award in 2013 from the IEEE Vehicular Technology Society, the Outstanding Paper Award from the IEEE AFICAN Conference in 2011, the Harvey N. Davis Teaching Award in 2003, the Jess H. Davis Memorial Award for excellence in research in 2001 from Stevens Institute of Technology, and the Sigma Xi Graduate Research Award from the University of Florida in 1999.

Braham Himed (F'07) received the Engineer degree in electrical engineering from Ecole Nationale Poly technique, Algiers, Algeria in 1984, and the M.S. and Ph.D. degrees both in electrical engineering, from Syracuse University, Syracuse, NY, USA, in 1987 and 1990, respectively. He is currently a Technical Advisor with the RF Technology Branch, Sensors Directorate, Air Force Research Laboratory, Dayton, OH, USA, where he is involved in several aspects of radar developments. His research interests include detection, estimation, multichannel adaptive signal processing, time series analyses, array processing, adaptive processing, waveform diversity, MIMO radar, passive radar, and over the horizon radar. He is the recipient of the 2001 IEEE region I award for his work on bistatic radar systems, algorithm development, and phenomenology and the 2012 IEEE Warren White Award for excellence in radar engineering. He is a Fellow of the AFRL (Class of 2013) and the Chair of the AESS Radar Systems Panel.